

WildSVG: Towards Reliable SVG Generation Under Real-Word Conditions

Marco Terral¹, Haotian Zhang^{1,2}, Tianyang Zhang¹, Meng Lin¹, Xiaoqing Xie¹
Haoran Dai^{1,3}, Darsh Kaushik^{1,4}, Pai Peng^{1,5}, Nicklas Scharpff¹, David Vazquez⁶, Joan Rodriguez^{1,4}

¹QuiverAI, ²Columbia University, ³Illinois Institute of Technology, ⁴Mila - Quebec Artificial Intelligence Institute, ⁵University of Wisconsin-Madison, ⁶ServiceNow Research

Abstract

We introduce the task of SVG extraction, which consists in translating specific visual inputs from an image into scalable vector graphics. Existing multimodal models achieve strong results when generating SVGs from clean renderings or textual descriptions, but they fall short in real-world scenarios where natural images introduce noise, clutter, and domain shifts. A central challenge in this direction is the lack of suitable benchmarks. To address this need, we introduce the WildSVG Benchmark, formed by two complementary datasets: Natural WildSVG, built from real images containing company logos paired with their SVG annotations, and Synthetic WildSVG, which blends complex SVG renderings into real scenes to simulate difficult conditions. Together, these resources provide the first foundation for systematic benchmarking SVG extraction. We benchmark state-of-the-art multimodal models and find that current approaches perform well below what is needed for reliable SVG extraction in real scenarios. Nonetheless, iterative refinement methods point to a promising path forward, and model capabilities are steadily improving.

1. Introduction

Scalable Vector Graphics (SVG) are an XML-based open standard and the leading format for vector graphic representation [30], widely adopted in modern image rendering. However, efficiently generating SVGs remains a significant challenge, as the format supports a wide range of primitives, from basic curves such as *path* to more complex shapes like *ellipse* or *polygon*. The task of image vectorization, producing SVG code from rendered images, remains unsolved by the industry. Traditional approaches rely on complex path operations, while deep learning methods struggle to generalize and often underutilize higher-level SVG primitives.

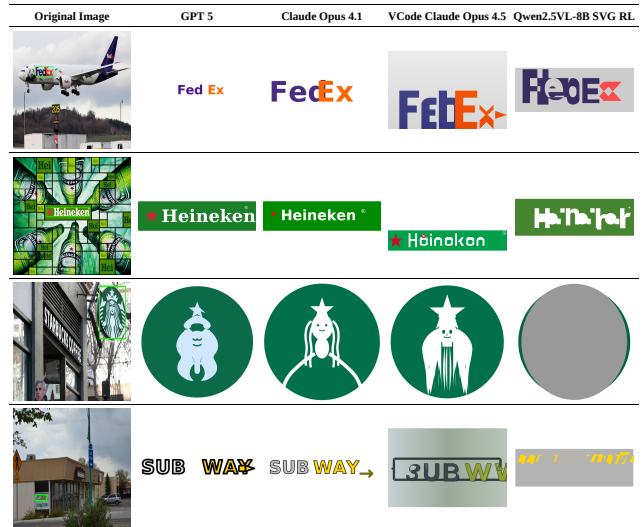


Figure 1. **Performance on WildSVG.** Extracting the logo from a real image and converting it to SVG using a two step pipeline. Comparison of VLMs on the WildSVG natural dataset.

Recent advances, such as StarVector [31], have demonstrated the potential of multimodal large language models (MLLMs) for SVG generation. StarVector trained on SVG-Stack, dataset of over two million samples, achieved state-of-the-art results through a reinforcement learning pipeline with visual feedback [32]. Despite this progress, existing methods are limited to controlled inputs such as clean renderings or text prompts. They fail when confronted with the challenges of natural images, where SVG elements are embedded in cluttered, noisy, and context-rich environments.

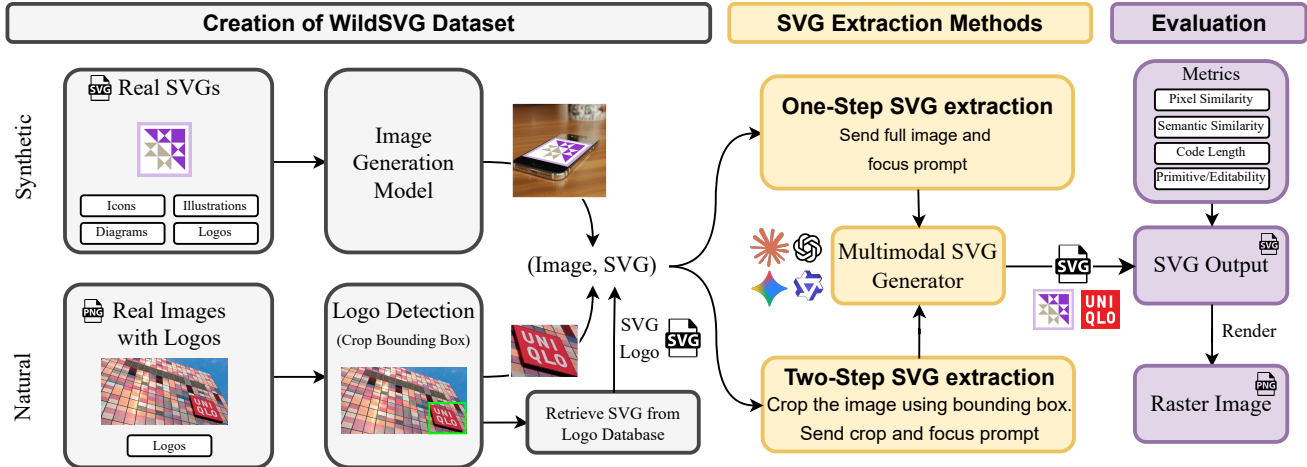


Figure 2. **Creation of the WildSVG Benchmark and evaluation pipeline.** The dataset combines a synthetic split, built by rendering real SVGs into generated scenes, and a natural split, created by detecting logos in real images and pairing them with SVG annotations. We evaluate SVG extraction using one step and two step multimodal methods and assess outputs through pixel similarity, semantic similarity, code quality, and editability metrics.

To address this gap, we introduce the SVG extraction task, which focuses on identifying graphical elements such as logos, icons, or pictograms within real-world images, given user guidance, and generating their corresponding SVG code. Unlike full-image vectorization, SVG extraction requires selective abstraction: isolating target elements while ignoring irrelevant visual content; as well as dealing with noises such as textures, shadows, occlusions, and perspective distortions that increase the difficulty of extracting the correct features.

We take three key steps to establish SVG extraction as a research problem. First, we introduce WildSVG, the first benchmark for this task, composed of two complementary datasets: (i) Natural WildSVG, which grounds vector annotations in real-world images, and (ii) Synthetic WildSVG, which embeds complex SVGs into natural scenes to simulate challenging visual conditions. Second, we define evaluation protocols to support consistent and fair benchmarking across models. Finally, we adopt multimodal models, with different training and inference approaches, as baselines, establishing initial performance levels and highlighting open challenges. Together, these steps lay the foundation for systematic study of SVG extraction.

2. Related work

Research on SVG generation is still in its early stages, with most work focused on reconstructing full graphics from clean renderings [31]. To the best of our knowledge, no prior work has addressed the SVG extraction task, isolating graphical elements from natural images and generating structured vector representations. Nevertheless, two research directions are closely related and inform our setting:

(1) logo detection, and (2) image-to-SVG generation.

2.1. Logo Detection and Extraction

Logo detection, a specialized form of object detection, has been widely studied due to applications in multimedia analysis, brand monitoring, and copyright protection. Early approaches relied on hand-crafted features combined with classifiers, while the rise of deep learning established detectors such as YOLO [22], DETR [6], and the R-CNN family [14] as the standard. Despite their success, these methods face challenges with dataset imbalance and the closed-set assumption, which limit their ability to generalize to unseen logos [17].

Recent work explores zero-shot and open-vocabulary detection to address these issues by leveraging language-vision alignment. For example, some methods replace fixed labels with textual descriptions [44], while others combine CLIP-based classifiers with object-agnostic detectors [34] or employ transformer-based region embeddings [13, 27]. Multimodal LLMs [2, 9, 11] further integrate such tasks into pretraining, extending them toward more context-aware object detection [42, 43]. However, these approaches output bounding boxes or class labels only, whereas SVG extraction requires both localization and structured vector code generation.

2.2. SVG Generation

Traditional vectorization methods rely on geometric fitting with the *path* primitive [29, 39, 40], often producing verbose SVG code with limited structural abstraction. Latent-variable models [5, 7, 19, 26] increase flexibility but are typically constrained to narrow SVG subsets and yield non-

Table 1. **Overview of publicly available logo detection datasets.** Existing datasets cover a wide range of logo classes, domains and scales, *yet all operate purely in the raster domain*. To the best of our knowledge, *no dataset provides paired SVG annotations*, highlighting the gap that WildSVG aims to fill.

Name	Classes	Images	Objects	Origin and Types
Belgalogos [20]	37	10,000	2,695	Photojournalist archives, general logos
FlickrLogos-27 [21]	27	1,080	4,671	General logos from Flickr search
FlickrLogos-32 [33]	32	2,240	5,644	General logos from Flickr search
SportLogo [23]	31	2,836	—	NHL and NBA logos from web search
Logos in the Wild [36]	871	11,054	32,850	Logos captured in diverse real scenes
QMUL OpenLogo [35]	352	27,083	—	Aggregation of 7 logo detection datasets
FoodLogoDet-1500 [16]	1,500	99,768	145,400	Logos from food industry products
LogoDet-3K [37]	3,000	158,652	194,261	General logos from large-scale web crawl

Table 2. **Overview of public SVG generation datasets.** Existing datasets provide large collections of SVGs across icons, fonts and diagrams, but none include natural image contexts or real world SVG extraction settings.

Dataset	Train	Val	Test	Primitives	Annotations
SVG Stack	2.1M	108k	5.7k	All	Captions
SVG Diagrams	—	—	472	All	Captions
SVG Fonts	1.8M	91.5k	4.8k	Vector paths	Font type
SVG Emoji	8.7k	667	668	All	Class
SVG Icons	80.4k	6.2k	2.4k	Vector paths	Class, caption

human-readable outputs.

Recent advances expand into specialized domains such as emoji generation [25, 38, 41], or employ LLMs for SVG creation and editing [3, 4], framing vector graphics as structured program synthesis [8, 12]. The most significant development is StarVector [31], which casts SVG generation as multimodal inverse rendering and code generation, trained on the large-scale SVG-Stack dataset. A posterior reinforcement learning extension, with rendering feedback (RLRF), further improved its visual fidelity [32]. Yet, these models remain restricted to clean renderings and degrade substantially in natural images with clutter, occlusion, or noise.

New studies also present ways for current state-of-the-art VLM (Visual Language Model), like GPT or Claude families, to deal with natural and photographic images for the SVG generation task. More specifically, VCode [24] proposes an iterative analysis and refinement of generated SVG, with usage of visual cues obtained from tools, in order to achieve symbolic SVG representations from images. This approach aims to extract the semantics from images and make a SVG representation faithful to it, rather than generate a high-fidelity SVG.

2.3. Dataset Survey

The task of identifying and processing SVG renderings within real-world images requires new datasets, *as none currently address this problem*. The StarVector paper [31] introduced SVG-Stack, along with several subsets, as resources for the Image-to-SVG task. While valuable, SVG-Stack focuses on clean renderings and does not capture the challenges of detecting and generating a SVG from natural contexts. Conversely, logo detection datasets provide only localization information (e.g., bounding boxes) without vector annotations.

We reviewed existing publicly available logo detection datasets (Tab. 1). Most provide bounding boxes in natural or semi-natural settings but lack vectorized logo representations. Among them, Logos-in-the-Wild stands out for its scale and diversity, covering difficult real-world conditions such as perspective distortion, scale variation, occlusion, and noisy textures. For SVG generation datasets, we focus on SVG-Stack and its subsets (Tab. 2), which remain the most comprehensive and high-quality resources for vector graphics research. However, they do not include SVGs embedded in real-world image contexts.

Taken together, no existing dataset satisfies the requirements of SVG extraction: grounding vector graphics within natural scenes while maintaining structured SVG annotations. This gap directly motivates the creation of our WildSVG dataset, introduced in the following section.

2.4. Motivation for SVG extraction

The SVG extraction tasks aim to cover a subset of SVG generation task in which a SVG integrated into an image must be extracted. The idea of this approach is to test models in their capacities to deal with complex noises while discriminating only specific elements. Prior work in logo de-

tection and SVG generation leaves a clear gap as neither tries to achieve this specific task. Detection models can localize target regions but cannot produce structured vector outputs, while SVG generation models excel on clean rasterized SVGs but fail in real-world conditions, where they have to render the demanded features inside challenging scenarios. The SVG extraction task bridges these domains, requiring both localization and vector generation. To enable systematic study of this task, we introduce the WildSVG benchmark, which provides the first datasets designed specifically for SVG extraction.

3. WildSVG Datasets

To enable systematic study of the SVG extraction task, we introduce the WildSVG datasets, consisting of two complementary datasets: Natural WildSVG and Synthetic WildSVG. Together, they combine the realism of naturally occurring logos with the diversity and controllability of synthetic SVG integration. The dataset generation pipelines are illustrated in the Appendix.

3.1. Natural WildSVG

Built from Logos-in-the-Wild [36], Natural WildSVG augments logo detections with vectorized annotations. Each bounding box is paired with (i) an SVG retrieved from worldvectorlogo.com, (ii) a textual description, and (iii) a focus prompt specifying the target element. To ensure consistency, candidate SVGs were validated using a VLM-based judging model and ranked by DINOv2 features similarity,[28], between rasterized SVGs and cropped detections. This process produced high-quality matches between natural logo appearances and their corresponding vector representations.

3.2. Synthetic WildSVG

To complement natural logos, Synthetic WildSVG integrates complex SVGs into realistic scenes. Starting from SVG-Stack [31], each SVG and its textual description were used to generate synthetic compositions with gemini-2.0-flash-preview-image-generation (now known as Nano Banana). Prompts were manually optimized to preserve SVG fidelity while embedding the logos naturally in the background. We additionally generated focus prompts for the complete dataset and manually annotated bounding boxes for the test split to support reliable evaluation. This dataset introduces diverse and complex SVG types under controlled but visually challenging conditions.

3.3. Quality filtering and resulting dataset

Both datasets underwent automated filtering inspired by StarVector-RL scoring system [32]. Each sample was scored on **constancy** (SVG-image similarity), **alignment** (focus prompt accuracy), and, for synthetic data, **aesthetics**

Table 3. **WildSVG** includes `Natural` samples where real images contain visible logos that are matched to their SVG versions, and `Synthetic` samples created by using image generation models to place each input SVG into a generated scene. The table reports sample counts, primitives and annotations.

Dataset	Train / Val / Test	Primitives	Annotations
Natural	12759 / 1418 / 227	Path	Logo brand, focus prompt, description, bounding box
Synthetic	2104 / 190 / 99	All	Focus prompt, description, bounding box (test only)

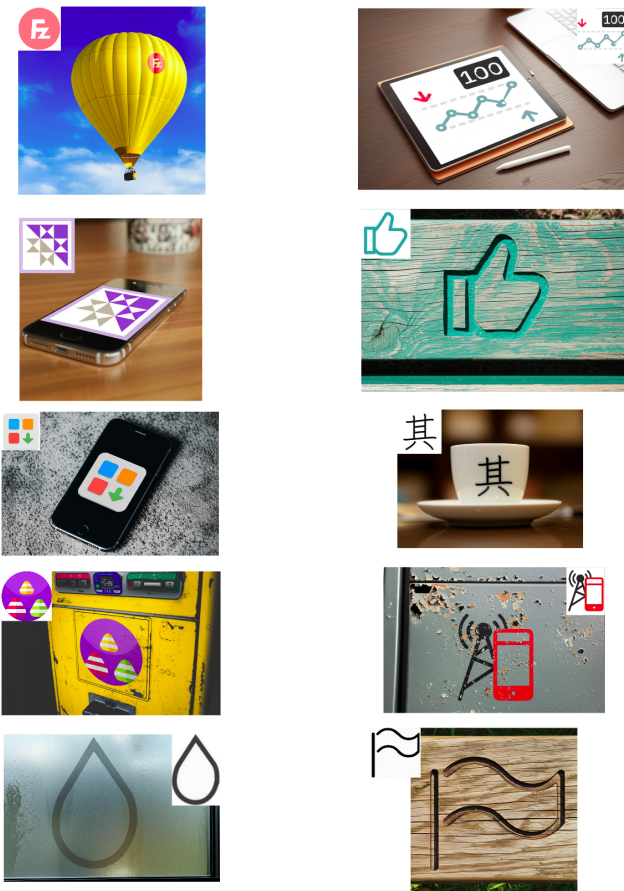


Figure 3. **Examples of Synthetic WildSVG.** Real SVGs extracted from SVG Stack are integrated into realistic scenarios using an image generation model.

(realism of integration). We combined these into aggregate scores and filtered them to at least a 5 out of 10 score, prioritizing constancy and aesthetics over alignment (details in Appendix). The resulting dataset statistics are shown in Tab. 3, further data about the test split can be found in the Appendix.

The final datasets are smaller than SVG-Stack or Logos-in-the-Wild, reflecting their intended use as fine-tuning and evaluation benchmarks rather than pretraining corpora. De-

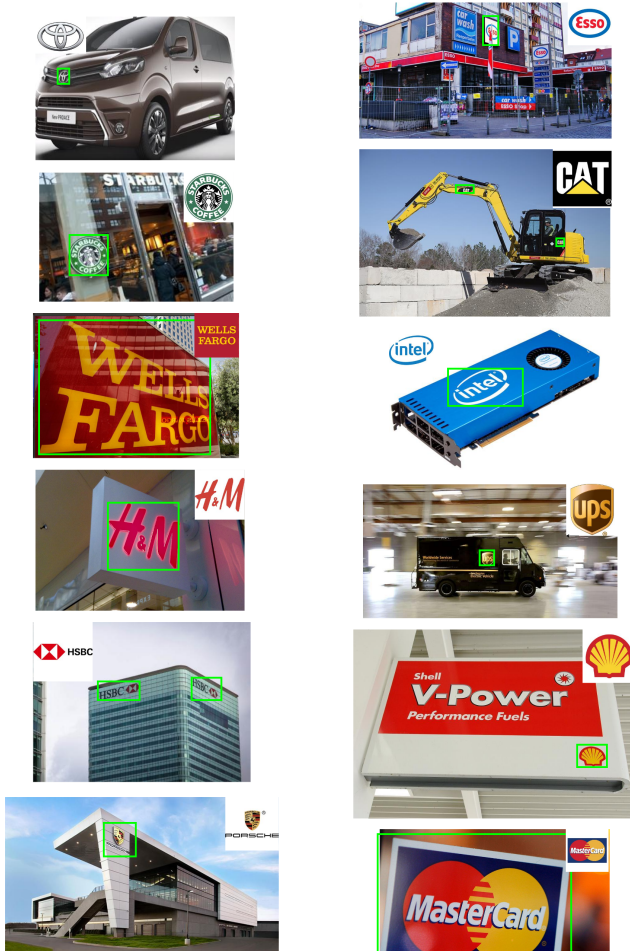


Figure 4. **Examples of Natural WildSVG.** Real images with visible logos are associated with the SVG logos that are extracted from public logo databases.

spite API constraints during synthetic generation, the resulting resources balance natural complexity and synthetic diversity, establishing WildSVG as the first benchmark for SVG extraction.

3.4. Licensing

The SVG-Stack data is released under a Creative Commons Attribution 4.0 International (CC BY 4.0) license. Accordingly, our Synthetic WildSVG extension is distributed under the same license, allowing both research and commercial use. In contrast, due to the copyrighted nature of images employed by Logos-in-the-Wild, the Natural WildSVG extension could only be licensed for research purposes.

4. WildSVG benchmark

The WildSVG benchmark aims to evaluate model performance on the SVG extraction task in both natural scenarios, which involve complex detections and real-world noise, and

synthetic scenarios, which feature simpler visual noise but more complex SVG structures. Employing the test split of each datasets.

4.1. Evaluation Metrics

To provide a meaningful assessment of the SVG extraction task, we evaluate models along four dimensions: pixel level fidelity, perceptual and semantic similarity, code compactness and editability. The metrics used are:

- **L2** and **SSIM** for pixel level fidelity,
- **LPIPS** [45] and **DINO score** [28] for perceptual and semantic similarity,
- **Token Length Difference** as a measure of code compactness [31], computed as the mean absolute difference between the ground truth SVGs and the generated ones to examine how long, or short, the responses are,
- **Primitive Diversity** which we propose as a proxy for SVG editability, since outputs built from a diverse set of simple primitives are easier to manipulate, restyle and modify at design time. It is computed as the average number of unique SVG primitives generated.

The use of multiple metrics is motivated by their complementary strengths. Pixel level fidelity metrics (L2, SSIM) capture precise reproduction of visual details, although they may penalize outputs that are perceptually faithful but not perfectly aligned at the pixel level. Perceptual and semantic metrics (LPIPS, DINO score) instead capture higher level similarity, complementing fidelity based measures. Code compactness and editability are also important for designers, since shorter and more primitive based SVGs are easier to manipulate and adapt.

4.2. Baselines

We benchmark a broad set of state-of-the-art multimodal model families on the SVG extraction task. The evaluated models include Qwen models (**Qwen2.5VL 72B Instruct** [2]), Gemini models (**Gemini 2.0 Flash** and **Gemini 2.5 Flash** [10]), Claude models (**Claude Opus 4** and **Claude Opus 4.1** [1]), GLM models (**GLM 4.1V 9B Thinking** and **GLM 4.5V** [15]), and GPT models (**GPT 4.1** and **GPT 5** [18]). We also evaluate an SVG specialized model, **Qwen2.5VL 8B SVG RL** trained with the SFT and RL pipeline introduced in StarVector and RLLRF (Reinforcement Learning from Rendering Feedback) [31, 32]. Finally, we test the a refinement-based method **VCode** [24] using Claude Sonnet 4.5.

Our goal is to analyze both the performance and trade-offs of each approach, both in one-shot model performance and more sophisticated refinement-based baselines.

4.3. Evaluation Setting

For a comprehensive evaluation, we conduct SVG extraction under two setups:

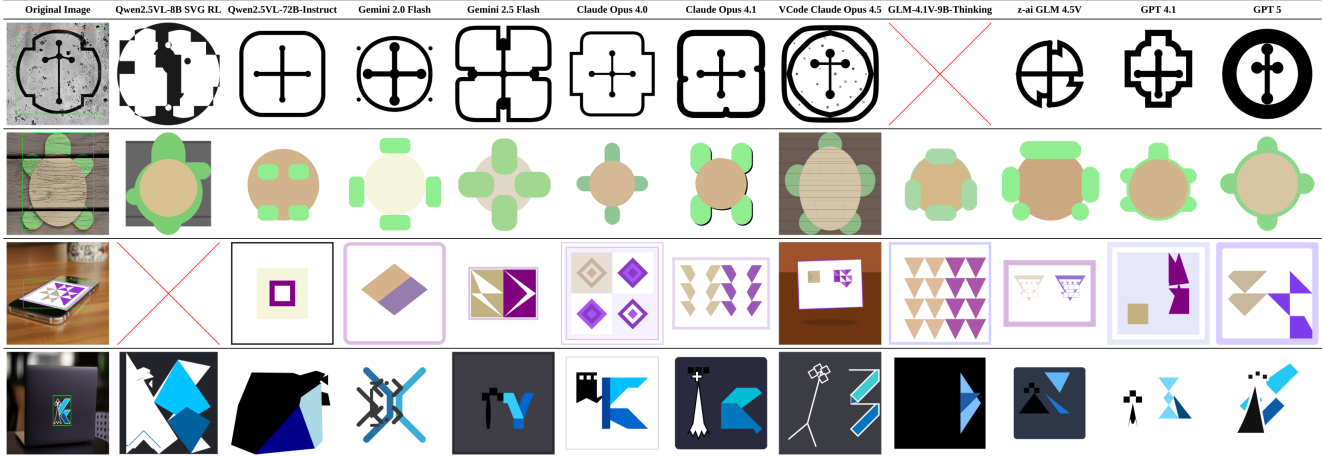


Figure 5. **Qualitative comparison of VLM outputs on the two step SVG extraction task using the Synthetic split.** Given the cropped logo from the detector, each model produces an SVG reconstruction. Results illustrate varying levels of geometric fidelity, color consistency, and structural correctness across models.

1. **Full-image Extraction with Focus Prompt:** The model receives the complete image along with a focus prompt that specifies the target element for extraction.
2. **Two-step Extraction with Perfect Object Localization:** Images are first cropped using perfect bounding boxes before SVG generation. This setting reduces distractions, helping models, particularly StarVector trained models, focus on specific features. It also serves as an upper bound for two-step methods that rely on external detection modules.

5. WildSVG Benchmark Results

From our current benchmark, we present reduced tables, containing the most recent model of each family; the complete results are provided in the Appendix. Since models within a family generally exhibit similar behavior, we focus on the most recent and best-performing representatives. We can also observe more qualitative results in the same previous section.

Two clear trends emerge from the results. First, across families, models produce SVGs that follow broadly similar patterns, with only a few notable outliers. Some outliers like Qwen2.5VL-8B RL SVG, frequently attempt to render the entire image rather than isolating the SVG. Other specific cases are the VCode inference, an approach used with Claude Sonnet 4.5, where we can see it render the background or some minor details, like the Star SVG in Fig. 7 or the Subway logo in Fig. 1. Second, models consistently achieve higher scores on the synthetic dataset, reflecting the greater difficulty of the natural dataset (more information in the Appendix); where scaling, perspective distortion, occlusions, shadows, and noise complicate vectorization. As shown in Fig. 6, even advanced models struggle with am-

biguous cases such as the Special K box, where only GPT 5 and VCode approach capture the “K” logo.

Observing Tab. 4, we can conclude that detection itself does not consistently improve results across families. The notable exception is Qwen2.5VL-8B SVG RL, trained with Starvector pipeline, which in the one-step setting ignores the prompt and attempts to vectorize the full image (Fig. 6). Despite the fact that other VLM families, including Qwen, do have the capacity to focus on the given prompt. This behavior suggests a weakness in StarVector’s training pipeline, as text-to-SVG and image-to-SVG tasks are learned separately in this regime which may reduce the alignment between prompt and image features during SVG generation.

Across families, **VLMs generally optimize for semantic similarity rather than aesthetic fidelity.** This tendency is reflected in the frequent use of the *text* primitive to approximate letters with similar fonts, rather than rendering them as shapes. As a result, SVGs achieve strong performance on semantic metrics (LPIPS, DINO) but weaker performance on pixel-level metrics (L2, SSIM). For example, the rendering of the Heineken logo in the GPT 5 model (Fig. 1) appears convincing in the overall structure but reveals clear inaccuracies upon closer examination. Synthetic examples further highlight this trade-off: some models reproduce SVGs with structures reminiscent of the original, but insufficiently faithful for precise extraction (Fig. 7, Fig. 8). This semantic approach generates simpler and shorter SVGs; in fact, the most accurate ones tend to be longer near the GT length, thus allowing for better expressivity. Despite Claude 4.1 and GPT 5 delivering the most semantically consistent and highest-fidelity SVG, both remain below the required threshold for a complete solution

Table 4. **Main results on WildSVG.** We report visual similarity metrics (DINO, LPIPS, L2, SSIM) and code metrics (length difference and primitive diversity) for one-step and two-step SVG extraction on the Natural and Synthetic splits. Lower is better for LPIPS, L2, and length difference. Higher is better for DINO, SSIM, and primitive diversity.

One-step generation												
Model	Natural						Synthetic					
	DINO ↑	LPIPS ↓	L2 ↓	SSIM ↑	Len diff ↓	Prim div ↑	DINO ↑	LPIPS ↓	L2 ↓	SSIM ↑	Len diff ↓	Prim div ↑
Qwen2.5VL 8B SVG RL	0.69	0.39	0.15	0.63	8108	2.57	0.76	0.43	<u>0.16</u>	<u>0.61</u>	10375	3.12
Qwen2.5VL 72B Instruct	0.77	0.41	0.22	0.58	8804	2.15	0.77	0.42	0.21	0.58	1516	1.86
GLM 4.5V	<u>0.79</u>	0.39	0.18	0.61	8710	2.02	0.77	<u>0.40</u>	0.19	0.59	1371	1.95
VCode Claude Sonnet 4.5	0.78	0.46	0.22	0.53	8141	<u>3.34</u>	0.85	0.38	0.20	0.59	<u>920</u>	2.66
Gemini Flash 2.5	0.79	0.42	0.20	0.58	<u>8509</u>	2.11	0.78	0.43	0.21	0.57	193	1.82
Claude Opus 4.1	0.80	0.40	<u>0.19</u>	<u>0.61</u>	8919	2.07	0.80	<u>0.42</u>	0.20	0.58	1441	2.03
GPT 5	0.80	0.40	<u>0.19</u>	0.58	6815	2.54	<u>0.79</u>	0.42	0.22	0.57	631	<u>2.21</u>

Two-step generation												
Model	Natural						Synthetic					
	DINO ↑	LPIPS ↓	L2 ↓	SSIM ↑	Len diff ↓	Prim div ↑	DINO ↑	LPIPS ↓	L2 ↓	SSIM ↑	Len diff ↓	Prim div ↑
Qwen2.5VL 8B SVG RL	0.74	0.46	<u>0.18</u>	0.60	<u>1323</u>	3.05	0.82	0.37	<u>0.16</u>	0.63	3063	3.20
VCode Claude Sonnet 4.5	0.77	0.58	0.30	0.45	7768	<u>3.04</u>	0.87	0.44	0.22	0.55	<u>690</u>	<u>2.90</u>
Qwen2.5VL 72B Instruct	0.81	0.36	0.21	0.62	8337	1.86	0.85	0.34	0.20	0.61	1484	1.99
GLM 4.5V	0.83	0.34	0.20	0.63	8302	1.98	0.86	<u>0.32</u>	0.18	0.64	1387	1.97
Gemini Flash 2.5	0.85	<u>0.32</u>	0.19	<u>0.64</u>	8669	2.06	0.88	0.33	0.19	<u>0.64</u>	1074	1.86
Claude Opus 4.1	<u>0.86</u>	0.32	0.16	0.66	8798	2.04	0.90	0.30	0.16	0.65	1405	2.00
GPT 5	0.87	0.34	0.18	0.63	6448	2.30	<u>0.89</u>	<u>0.31</u>	<u>0.18</u>	<u>0.63</u>	921	2.13

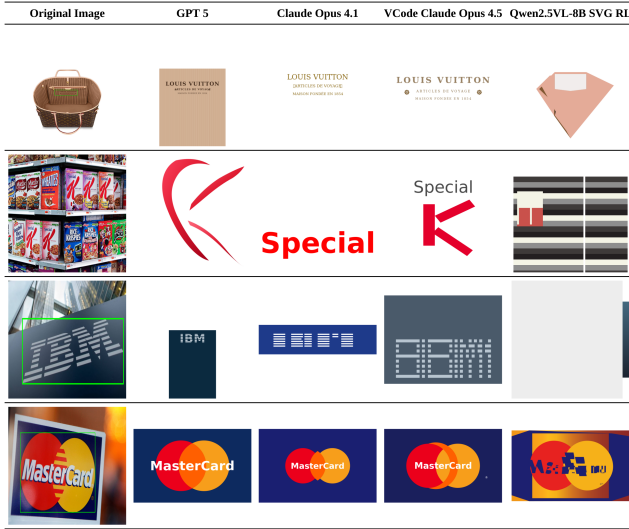


Figure 6. Comparison of VLMs for one-step SVG extraction natural dataset

of SVG extraction.

Qwen2.5VL-8B SVG RL and VCode diverge from this general trend, sacrificing semantic fidelity in favor of visual aesthetics. This is reflected in the metrics, where L2 and SSIM are prioritized over LPIPS and DINO, and in qualitative examples such as the FedEx and Heineken logos (Fig. 1). In these cases, they often rely on shape primitives to render letters, a strategy preferable to text primitives since reproducing exact font styles, kerning, and spacing is effectively impossible. While this approach reduces

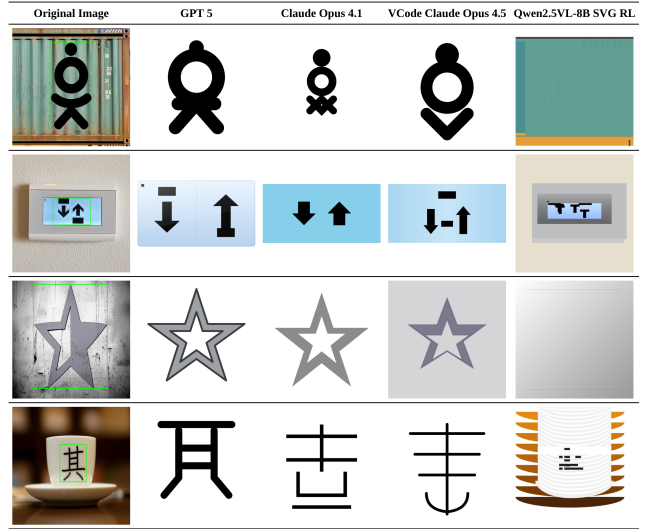


Figure 7. Comparison of VLMs for one-step SVG extraction synthetic dataset

semantic scores, it has the potential to produce SVGs visually closer to the original designs. Another effect of this approach is that the generated SVGs tend also to be longer and more expressive with primitives (to the detriment of Qwen2.5VL-8B SVG RL and improving VCode length metrics); this makes intuitive sense, employing more primitives might help achieve complex structures but is expensive with tokens. However, *for the specific task of SVG extraction, Qwen2.5VL-8B SVG RL's results remain below the semantic and aesthetic quality achieved by Claude and GPT*

models, even when solving its alignment problem by providing a detected SVG. We hypothesize that noise in real-world scenarios, such as textures and shadows, may overwhelm the model, leading it to overfit to subtle visual variations rather than isolating the core SVG structures. And thus explaining why this model still shows strong capabilities in generating complex code directly from rasterized SVGs. However the VCode approach shows greater potential, providing similar SVG extraction approaches while improving on its failures. With VCode inference we are able to increase the performance of Claude Sonnet 4.5, Tab. 4, while maintaining the focusing capacities of the model. We can also observe the same philosophy of SVGs with greater potential for accuracy while providing more semantical readability. On top of that these SVGs aren't as long while maintaining the primitive diversity.

Overall, our baseline demonstrates that current VLMs can generate simpler SVGs that are semantically meaningful but still fall short in aesthetic fidelity and primitive potential. Across families, most models achieve relatively similar scores regardless of the visual encoder or LLM architecture, suggesting that model size and inference technique play a greater role than design choices. As Open-source models, typically ranging from 10–70B parameters, tend to perform slightly worse than larger proprietary systems. However, even the strongest models, such as Claude 4.1 and GPT 5, plateau at approximately DINO 90, LPIPS 30, SSIM 60, and L2 15. Even employing more complex inference approaches like VCode. By comparison, achieving high-fidelity SVG generation would require scores closer to DINO 95, LPIPS 10, SSIM 80, and L2 9. In fact, our code metrics indicate an under usage of tokens and primitives, clearly illustrated in the qualitative results. These findings point to a performance ceiling in current approaches which still require to be addressed.

6. Conclusion

We introduced the task of SVG extraction, extending multi-modal models to generate vector graphics directly from natural images, and proposed WildSVG, the first benchmark for this problem. WildSVG combines real-world logos with synthetic compositions, enabling evaluation under both natural and controlled conditions.

Our benchmarking of leading VLM families reveals three consistent takeaways: (1) models perform better on synthetic than natural data, showing the impact of real-world distortions; (2) current systems prioritize semantic similarity over pixel fidelity; (3) even the strongest models plateau below high-fidelity thresholds, leaving clear headroom for improvement. While Claude and GPT balance fidelity and semantics most effectively, Qwen2.5VL-8B SVG RL highlights a contrasting trade-off by favoring aesthetics over semantics while still lacking to achieve competitive

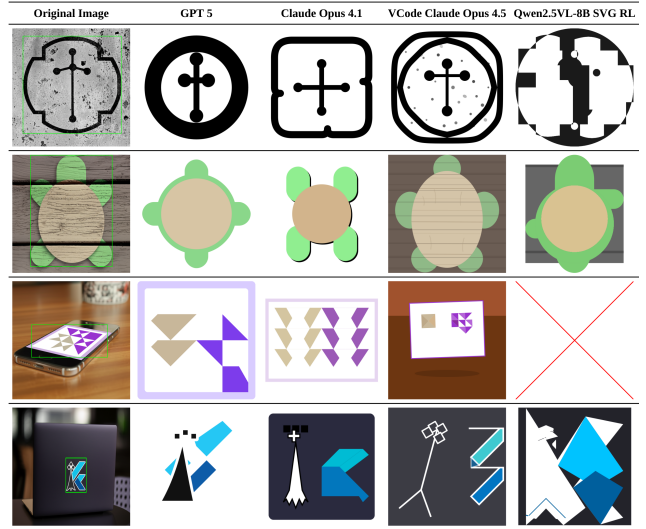


Figure 8. Comparison of VLMs for two-step SVG extraction synthetic dataset

performance. Iterative inference show promising results if combined with a strong VLM.

Looking ahead, we identify several open research directions: (i) improving alignment between prompts and structured vector outputs, particularly for StarVector training; (ii) integrating SVG generation and extraction tasks into VLM training pipelines to improve fidelity in vector code; (iii) extending two-step approaches to leverage SVG generation without requiring task-specific fine-tuning; (iiii) study the impact of iterative approaches in better trained model; and (iiiiii) expanding WildSVG datasets to allow broader training approaches not only finetuning.

By framing SVG extraction as a benchmarked task, we aim to catalyze future research at the intersection of vision, language, and structured graphics generation.

References

- [1] The claude 3 model family: Opus, sonnet, haiku. 2025. 5
- [2] Shuai Bai, Keqin Chen, Xuejing Liu, Jialin Wang, Wenbin Ge, Sibao Song, Kai Dang, Peng Wang, Shijie Wang, Jun Tang, Humen Zhong, Yuanzhi Zhu, Mingkun Yang, Zhaohai Li, Jianqiang Wan, Pengfei Wang, Wei Ding, Zheren Fu, Yiheng Xu, Jiabo Ye, Xi Zhang, Tianbao Xie, Zesen Cheng, Hang Zhang, Zhibo Yang, Haiyang Xu, and Junyang Lin. Qwen2.5-vl technical report, 2025. 2, 5
- [3] Sébastien Bubeck, Varun Chandrasekaran, Ronen Eldan, Johannes Gehrke, Eric Horvitz, Ece Kamar, Peter Lee, Yin Tat Lee, Yuanzhi Li, Scott Lundberg, Harsha Nori, Hamid Palangi, Marco Tulio Ribeiro, and Yi Zhang. Sparks of artificial general intelligence: Early experiments with gpt-4, 2023. 3
- [4] Mu Cai, Zeyi Huang, Yuheng Li, Utkarsh Ojha, Haohan Wang, and Yong Jae Lee. Leveraging large language mod-

- els for scalable vector graphics-driven image understanding, 2024. 3
- [5] Defu Cao, Zhaowen Wang, and Jose Ignacio Echevarria Vallespi. Representation learning for continuous vector graphics, 2024. 2
- [6] Nicolas Carion, Francisco Massa, Gabriel Synnaeve, Nicolas Usunier, Alexander Kirillov, and Sergey Zagoruyko. End-to-end object detection with transformers, 2020. 2
- [7] Alexandre Carlier, Martin Danelljan, Alexandre Alahi, and Radu Timofte. Deepsvg: A hierarchical generative network for vector graphics animation, 2020. 2
- [8] Mark Chen, Jerry Tworek, Heewoo Jun, and etc.. Evaluating large language models trained on code, 2021. 3
- [9] Xi Chen, Josip Djolonga, Piotr Padlewski, Basil Mustafa, Soravit Changpinyo, Jialin Wu, Carlos Riquelme Ruiz, Sebastian Goodman, Xiao Wang, Yi Tay, Siamak Shakeri, Mostafa Dehghani, Daniel Salz, Mario Lucic, Michael Tschannen, Arsha Nagrani, Hexiang Hu, Mandar Joshi, Bo Pang, Ceslee Montgomery, Paulina Pietrzyk, Marvin Ritter, AJ Piergiovanni, Matthias Minderer, Filip Pavetic, Austin Waters, Gang Li, Ibrahim Alabdulmohsin, Lucas Beyer, Julien Amelot, Kenton Lee, Andreas Peter Steiner, Yang Li, Daniel Keysers, Anurag Arnab, Yuanzhong Xu, Keran Rong, Alexander Kolesnikov, Mojtaba Seyedhosseini, Anelia Angelova, Xiaohua Zhai, Neil Houlsby, and Radu Soricut. Pali-x: On scaling up a multilingual vision and language model, 2023. 2
- [10] Gheorghe Comanici, Eric Bieber, Mike Schaekermann, Ice Pasupat, Noveen Sachdeva, Inderjit Dhillon, Marcel Blstein, Ori Ram, Dan Zhang, Evan Rosen, et al. Gemini 2.5: Pushing the frontier with advanced reasoning, multimodality, long context, and next generation agentic capabilities. *arXiv preprint arXiv:2507.06261*, 2025. 5
- [11] Matt Deitke, Christopher Clark, Sangho Lee, Rohun Tripathi, Yue Yang, Jae Sung Park, Mohammadreza Salehi, Niklas Muennighoff, Kyle Lo, Luca Soldaini, Jiasen Lu, Taira Anderson, Erin Bransom, Kiana Ehsani, Huong Ngo, YenSung Chen, Ajay Patel, Mark Yatskar, Chris Callison-Burch, Andrew Head, Rose Hendrix, Favyen Bastani, Eli VanderBilt, Nathan Lambert, Yvonne Chou, Arnavi Chheda, Jenna Sparks, Sam Skjonsberg, Michael Schmitz, Aaron Sarnat, Byron Bischoff, Pete Walsh, Chris Newell, Piper Wolters, Tanmay Gupta, Kuo-Hao Zeng, Jon Borchardt, Dirk Groeneveld, Crystal Nam, Sophie Lebrecht, Caitlin Wittlif, Carissa Schoenick, Oscar Michel, Ranjay Krishna, Luca Weihs, Noah A. Smith, Hannaneh Hajishirzi, Ross Girshick, Ali Farhadi, and Aniruddha Kembhavi. Molmo and pixmo: Open weights and open data for state-of-the-art vision-language models, 2024. 2
- [12] Zhangyin Feng, Daya Guo, Duyu Tang, Nan Duan, Xiaocheng Feng, Ming Gong, Linjun Shou, Bing Qin, Ting Liu, Daxin Jiang, and Ming Zhou. Codebert: A pre-trained model for programming and natural languages, 2020. 3
- [13] Xiuye Gu, Tsung-Yi Lin, Weicheng Kuo, and Yin Cui. Open-vocabulary object detection via vision and language knowledge distillation, 2022. 2
- [14] Kaiming He, Georgia Gkioxari, Piotr Dollár, and Ross Girshick. Mask r-cnn, 2018. 2
- [15] Wenyi Hong, Wenmeng Yu, Xiaotao Gu, Guo Wang, Guobing Gan, Haomiao Tang, Jiale Cheng, Ji Qi, Junhui Ji, Li-hang Pan, et al. Glm-4.1 v-thinking: Towards versatile multimodal reasoning with scalable reinforcement learning. *arXiv e-prints*, pages arXiv-2507, 2025. 5
- [16] Qiang Hou, Weiqing Min, Jing Wang, Sujuan Hou, Yuanjie Zheng, and Shuqiang Jiang. Foodlogodet-1500: A dataset for large-scale food logo detection via multi-scale feature decoupling network. In *Proceedings of the 29th ACM International Conference on Multimedia*, page 4670–4679, New York, NY, USA, 2021. Association for Computing Machinery. 3
- [17] Sujuan Hou, Jiacheng Li, Weiqing Min, Qiang Hou, Yanna Zhao, Yuanjie Zheng, and Shuqiang Jiang. Deep learning for logo detection: A survey. *ACM Trans. Multimedia Comput. Commun. Appl.*, 20(3), 2023. 2
- [18] Aaron Hurst, Adam Lerer, Adam P Goucher, Adam Perelman, Aditya Ramesh, Aidan Clark, AJ Ostrow, Akila Welihinda, Alan Hayes, Alec Radford, et al. Gpt-4o system card. *arXiv preprint arXiv:2410.21276*, 2024. 5
- [19] Ajay Jain, Amber Xie, and Pieter Abbeel. Vectorfusion: Text-to-svg by abstracting pixel-based diffusion models, 2022. 2
- [20] Alexis Joly and Olivier Buisson. Logo retrieval with a contrario visual query expansion. In *Proceedings of the 17th ACM International Conference on Multimedia*, page 581–584, New York, NY, USA, 2009. Association for Computing Machinery. 3
- [21] Yannis Kalantidis, Lluís Garcia Pueyo, Michele Trevisiol, Roelof van Zwol, and Yannis Avrithis. Scalable triangulation-based logo recognition. In *Proceedings of the 1st ACM International Conference on Multimedia Retrieval*, New York, NY, USA, 2011. Association for Computing Machinery. 3
- [22] Rahima Khanam and Muhammad Hussain. Yolov11: An overview of the key architectural enhancements, 2024. 2
- [23] Andrey Kuznetsov and Andrey V. Savchenko. A new sport teams logo dataset for detection tasks. In *Computer Vision and Graphics*, pages 87–97, Cham, 2020. Springer International Publishing. 3
- [24] Kevin Qinghong Lin, Yuhao Zheng, Hangyu Ran, Dantong Zhu, Dongxing Mao, Linjie Li, Philip Torr, and Alex Jinpeng Wang. Vcode: a multimodal coding benchmark with svg as symbolic visual representation, 2025. 3, 5
- [25] Raphael Gontijo Lopes, David Ha, Douglas Eck, and Jonathon Shlens. A learned representation for scalable vector graphics, 2019. 3
- [26] Xu Ma, Yuqian Zhou, Xingqian Xu, Bin Sun, Valerii Filev, Nikita Orlov, Yun Fu, and Humphrey Shi. Towards layer-wise image vectorization, 2022. 2
- [27] Matthias Minderer, Alexey Gritsenko, Austin Stone, Maxim Neumann, Dirk Weissenborn, Alexey Dosovitskiy, Aravindh Mahendran, Anurag Arnab, Mostafa Dehghani, Zhuoran Shen, Xiao Wang, Xiaohua Zhai, Thomas Kipf, and Neil Houlsby. Simple open-vocabulary object detection. In *Computer Vision – ECCV 2022*, pages 728–755, Cham, 2022. Springer Nature Switzerland. 2

- [28] Maxime Oquab, Timothée Darcet, Theo Moutakanni, Huy V. Vo, Marc Szafranec, Vasil Khalidov, Pierre Fernandez, Daniel Haziza, Francisco Massa, Alaaeldin El-Nouby, Russell Howes, Po-Yao Huang, Hu Xu, Vasu Sharma, Shang-Wen Li, Wojciech Galuba, Mike Rabbat, Mido Assran, Nicolas Ballas, Gabriel Synnaeve, Ishan Misra, Herve Jegou, Julien Mairal, Patrick Labatut, Armand Joulin, and Piotr Bojanowski. Dinov2: Learning robust visual features without supervision, 2023. [4](#), [5](#)
- [29] Sanford Pun and Chris Tang. Vision cortex. vtracer, 2025. [2](#)
- [30] Antoine Quint. Scalable vector graphics. *IEEE MultiMedia*, 10(3):99–102, 2003. [1](#)
- [31] Juan A. Rodriguez, Abhay Puri, Shubham Agarwal, Issam H. Laradji, Pau Rodriguez, Sai Rajeswar, David Vazquez, Christopher Pal, and Marco Pedersoli. Starvector: Generating scalable vector graphics code from images and text, 2025. [1](#), [2](#), [3](#), [4](#), [5](#)
- [32] Juan A. Rodriguez, Haotian Zhang, Abhay Puri, Aarash Feizi, Rishav Pramanik, Pascal Wichmann, Arnab Mondal, Mohammad Reza Samsami, Rabiul Awal, Perouz Taslakian, Spandana Gella, Sai Rajeswar, David Vazquez, Christopher Pal, and Marco Pedersoli. Rendering-aware reinforcement learning for vector graphics generation, 2025. [1](#), [3](#), [4](#), [5](#)
- [33] Stefan Romberg, Lluís Garcia Pueyo, Rainer Lienhart, and Roelof van Zwol. Scalable logo recognition in real-world images. In *Proceedings of the 1st ACM International Conference on Multimedia Retrieval*, New York, NY, USA, 2011. Association for Computing Machinery. [3](#)
- [34] Mikhail Shulgin and Ilya Makarov. Scalable zero-shot logo recognition. *IEEE Access*, 11:142702–142710, 2023. [2](#)
- [35] Hang Su, Xiatian Zhu, and Shaogang Gong. Open logo detection challenge, 2018. [3](#)
- [36] Andras Tüzkö, Christian Herrmann, Daniel Manger, and Jürgen Beyerer. Open set logo detection and retrieval, 2017. [3](#), [4](#)
- [37] Jing Wang, Weiqing Min, Sujuan Hou, Shengnan Ma, Yuanjie Zheng, and Shuqiang Jiang. Logodet-3k: A large-scale image dataset for logo detection. *ACM Trans. Multimedia Comput. Commun. Appl.*, 18(1), 2022. [3](#)
- [38] Yizhi Wang and Zhouhui Lian. Deepvecfont: Synthesizing high-quality vector fonts via dual-modality learning, 2021. [3](#)
- [39] Martin Weber. Autotrace, 2025. [2](#)
- [40] Ronghuan Wu, Wanchao Su, Kede Ma, and Jing Liao. Iconshop: Text-guided vector icon synthesis with autoregressive transformers, 2023. [2](#)
- [41] Ronghuan Wu, Wanchao Su, Kede Ma, and Jing Liao. Iconshop: Text-guided vector icon synthesis with autoregressive transformers, 2023. [3](#)
- [42] Heng Yin, Yuqiang Ren, Ke Yan, Shouhong Ding, and Yongtao Hao. Rod-mlm: Towards more reliable object detection in multimodal large language models. In *Proceedings of the Computer Vision and Pattern Recognition Conference (CVPR)*, pages 14358–14368, 2025. [2](#)
- [43] Yuhang Zang, Wei Li, Jun Han, Kaiyang Zhou, and Chen Change Loy. Contextual object detection with multimodal large language models. *International Journal of Computer Vision*, 133(2):825–843, 2025. [2](#)
- [44] Alireza Zareian, Kevin Dela Rosa, Derek Hao Hu, and Shih-Fu Chang. Open-vocabulary object detection using captions, 2021. [2](#)
- [45] Richard Zhang, Phillip Isola, Alexei A Efros, Eli Shechtman, and Oliver Wang. The unreasonable effectiveness of deep features as a perceptual metric. In *CVPR*, 2018. [5](#)

WildSVG: Towards Reliable SVG Generation Under Real-Word Conditions

Supplementary Material

7. Appendix

7.1. LLM usage

Parts of this manuscript were refined and polished using ChatGPT (GPT-5), a large language model developed by OpenAI. The model was employed solely for language editing and clarity improvements; all technical content, data analyses, and conceptual contributions remain the original work of the authors.

7.2. Complete benchmark

In Tab. 5 we report the benchmark results for all VLMs evaluated in our study.

7.3. Dataset generation

7.3.1. Dataset generation pipelines

We present in Fig. 9 and Fig. 10 the processing pipelines employed for generating the WildSVG datasets. In Fig. 11 we can observe the prompt employed in the synthetic WildSVG dataset pipeline for integrating SVGs into images. This prompt was generated manually after multiple iterations, achieving the most aesthetic pleasing results while maintaining most or all the features of the original SVG.

We also present the prompts employed for VLM judging the instance of each dataset, Fig. 12 and Fig. 13.

7.3.2. Filtering score formulas

The filtering procedure was performed using the following equations: Eq. (1) and Eq. (2).

$$\text{Synthetic Dataset Score} = 40\% \cdot C_{\text{score}} + 40\% \cdot AE_{\text{score}} + 20\% \cdot AL_{\text{score}}, \quad (1)$$

$$\text{Natural Dataset Score} = 60\% \cdot C_{\text{score}} + 40\% \cdot AL_{\text{score}}. \quad (2)$$

7.3.3. Dataset statistics

As shown in Fig. 14, the heatmap reveals a more diverse spatial distribution of bounding boxes in the natural dataset, while the synthetic dataset exhibits a strong central bias. This observation motivated our decision to increase the weight of WildSVG for these detections, specifically to mitigate this type of positional bias.

From Fig. 15, we observe that bounding boxes in the natural dataset tend to be smaller, with a clear skew toward reduced sizes. In contrast, the synthetic dataset displays a more uniform distribution of bounding box dimensions. In the synthetic case, the mean and median sizes are both

around 0.5, which generally makes SVG detection easier. The combination of smaller bounding boxes and greater positional variability makes the natural dataset inherently more challenging, especially when real world noise is also considered.

Examining the score distributions in Fig. 16 reveals several additional points. Overall, both datasets exhibit reasonable alignment scores. However, the natural dataset shows slightly lower consistency compared with the synthetic one. This can be attributed to the fact that real world logos often contain small variations, so even when an SVG is conceptually similar, minor differences in color or spatial layout make exact matches harder to retrieve from the database. The aesthetic scores of the synthetic dataset also indicate that SVG integration can still be improved, since the distribution remains centered around a medium score of about 3 out of 5.

7.3.4. Additional qualitative results on WildSVG

We present more results of the different SVG extraction approaches and models; Fig. 17, Fig. 18 and Fig. 19.

7.3.5. WildSVG Dataset

We present further examples from WildSVG dataset in Fig. 20 and Fig. 21.

Table 5. **Complete unified results on WildSVG.** We include the diverse families and versions benchmarked on WildSVG, including both the one-step and two-step SVG extraction on the Natural and Synthetic splits.

One-step generation												
Model	Natural						Synthetic					
	DINO ↑	LPIPS ↓	L2 ↓	SSIM ↑	Len diff ↓	Prim div ↑	DINO ↑	LPIPS ↓	L2 ↓	SSIM ↑	Len diff ↓	Prim div ↑
Qwen2.5VL-72B-Instruct	0.77	0.41	0.22	0.58	8803.83	2.15	0.77	0.42	0.21	0.58	1516.36	1.86
Qwen2.5VL-8B SVG RL	0.69	0.39	0.15	0.63	8108.38	<u>2.57</u>	0.76	0.43	0.16	0.61	10374.72	3.12
Gemini Flash 2	0.78	<u>0.38</u>	<u>0.17</u>	<u>0.61</u>	8233.99	1.69	0.83	0.32	0.19	<u>0.63</u>	1202.83	1.51
Gemini Flash 2.5	0.79	0.42	0.20	0.58	8509.60	2.11	0.78	0.43	0.21	0.57	192.90	1.82
Claude Opus 4	0.78	0.40	0.18	0.60	8895.15	2.35	0.84	<u>0.34</u>	0.19	0.62	1395.59	2.17
Claude Opus 4.1	<u>0.80</u>	0.40	0.19	<u>0.61</u>	8919.63	2.07	0.80	0.42	0.20	0.58	1441.08	2.03
VCode Claude Sonnet 4.5	0.78	0.46	0.22	0.53	8140.55	3.34	<u>0.85</u>	0.38	0.20	0.59	920.07	2.66
GLM-4.1V-9B-Thinking	0.75	0.37	<u>0.17</u>	0.63	8954.52	2.13	0.78	0.37	0.21	0.62	1295.58	1.87
z-ai GLM 4.5V	0.79	0.39	0.18	<u>0.61</u>	8710.47	2.02	0.77	0.40	0.19	0.59	1370.70	1.95
GPT 4.1	0.81	0.39	0.18	0.59	8775.49	2.18	0.86	0.32	<u>0.18</u>	0.64	1237.15	1.93
GPT 5	<u>0.80</u>	0.40	0.19	0.58	6814.91	2.54	0.79	0.42	0.22	0.57	630.88	2.21

Two-step generation												
Model	Natural						Synthetic					
	DINO ↑	LPIPS ↓	L2 ↓	SSIM ↑	Len diff ↓	Prim div ↑	DINO ↑	LPIPS ↓	L2 ↓	SSIM ↑	Len diff ↓	Prim div ↑
Qwen2.5VL-72B-Instruct	0.81	0.36	0.21	0.62	8337.19	1.86	0.85	0.34	0.20	0.61	1483.57	1.99
Qwen2.5VL-8B SVG RL	0.74	0.46	0.18	0.60	1323.05	3.05	0.82	0.37	0.16	0.63	3062.99	3.20
Gemini Flash 2	0.76	0.40	0.18	0.61	8328.87	1.58	0.86	0.32	0.18	0.64	1307.80	1.65
Gemini Flash 2.5	0.85	0.32	0.19	0.64	8668.80	2.06	0.88	0.33	0.19	0.64	1074.12	1.86
Claude Opus 4	0.78	0.43	0.19	0.58	8647.89	2.16	0.88	0.30	0.15	0.66	1352.99	2.08
Claude Opus 4.1	0.86	0.32	0.16	0.66	8797.66	2.04	0.90	0.30	0.16	0.65	1405.42	2.00
VCode Claude Sonnet 4.5	0.77	0.58	0.30	0.45	7767.66	3.04	0.87	0.44	0.22	0.55	689.90	2.90
GLM-4.1V-9B-Thinking	0.76	0.41	0.20	0.59	8488.48	1.89	0.83	0.33	0.18	0.63	1327.17	1.90
z-ai GLM 4.5V	0.83	0.34	0.20	0.63	8301.63	1.98	0.86	0.32	0.18	0.64	1386.77	1.97
GPT 4.1	0.80	0.41	0.20	0.57	8779.01	2.01	0.88	0.31	0.17	0.63	1475.92	2.04
GPT 5	0.87	0.34	0.18	0.63	6448.23	2.30	0.89	0.31	0.18	0.63	921.46	2.13

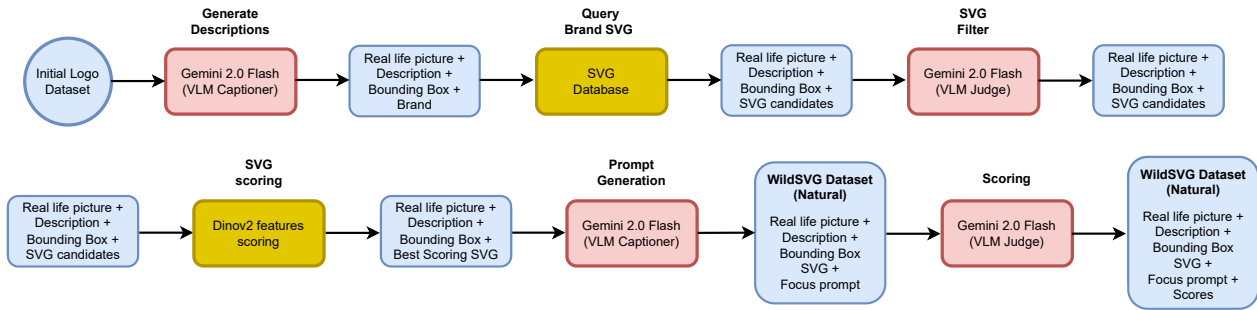


Figure 9. Pipeline for synthetic WildSVG generation

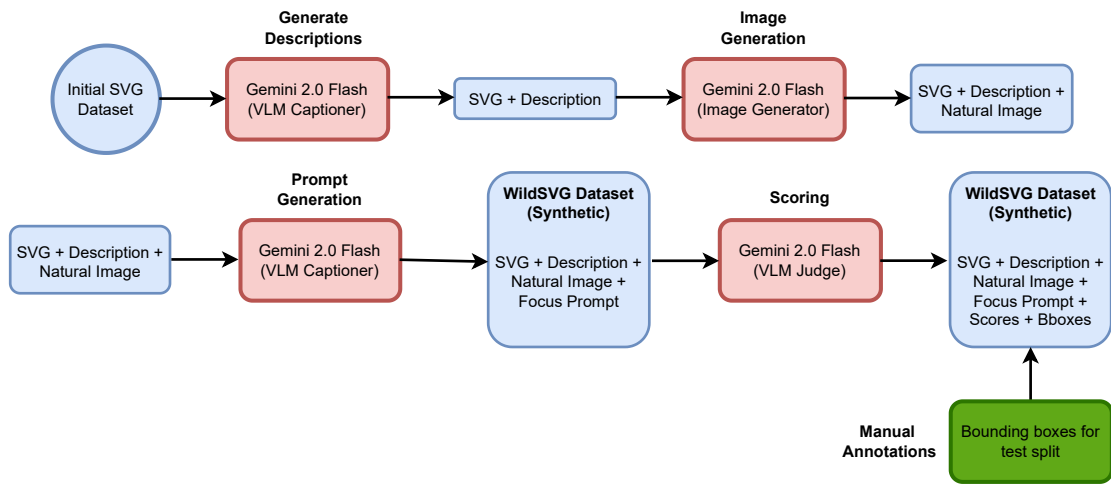


Figure 10. Pipeline for natural WildSVG generation

Prompt for Synthetic Image Generation

Integrate the image into a **real life photography** to help increase **difficulty** on a **dataset**. It must be **seamless** and the **integrated image** in the real life picture should **respect** the following **description**: (description). First, decide on a **scenario** where to apply this SVG, it must be **semantically consistent**. An example could be a **publicity panel** or a **traffic sign** or a logo in a laptop, it is highly **encouraged** to think about **others scenarios**.

Figure 11. Prompt for image generation of Synthetic WildSVG Dataset

Prompt for VLLM scoring (Natural dataset)

You are a strict impartial evaluator of integrating SVG images into real life scenarios.

RUBRIC

Constancy Score (0-5) — How similar is the integrated image, does it maintain the original characteristics or does it remove them or add new things, without taking into account perspective or scale changes.

0 — **Completely unrecognizable**: Completely changed image.

1 — **Very weak recognition**: Some minor features are present but lack in key characteristics which makes it barely recognizable.

2 — **Weak recognition**: Some primary characteristics are present but other key features are missing or completely changed. Very difficult to recognize as the integrated pictures.

3 — **Partial recognition**: Most important features are present, but some minor details or more secondary characteristics are missing or have being noticeable altered or newly added.

4 — **Strong recognition**: Recognizable, only some slight changes or addition in minor details have been done.

5 — **Perfect recognition**: Image is fully integrated with every minor detail conserved.

Alignment Score (0-5) — "How well adjusted is the information of a task prompt about the location of the integrated picture and what to extract."

0 — **Unusable**: Completely wrong location or completely wrong information about what to extract.

1 — **Very poor**: Difficult to understand or very ambiguous on what should be extracted.

2 — **Poor**: Somehow correct but confusing or ambiguous.

3 — **Fair**: Basic information without any class of details or additional information to deal with ambiguity.

4 — **Good**: Clear location and what to extract although some details are missing, leaving the possibility of some ambiguity.

5 — **Excellent**: Excellent information, clear and distinct leaving no room for ambiguity on what to extract.

TASK

Given the two images, one integrated into the other, and a task prompt with location information evaluate using the rubric; return the following JSON:

```
{
  "constancy_score": <integer 0-5>,
  "alignment_score": <integer 0-5>,
  "justification": 100-word explanation for each score
}
```

Figure 12. Prompt for scoring Natural WildSVG instances

Prompt for VLLM scoring (Synthetic dataset)

You are a strict impartial evaluator of integrating SVG images into real life scenarios.

RUBRIC

Constancy Score (0-5) — How similar is the integrated image, does it maintain the original characteristics or does it remove them or add new things, without taking into account perspective or scale changes.

0 — **Completely unrecognizable**: Completely changed image.

1 — **Very weak recognition**: Some minor features are present but lack in key characteristics which makes it barely recognizable.

2 — **Weak recognition**: Some primary characteristics are present but other key features are missing or completely changed. Very difficult to recognize as the integrated pictures.

3 — **Partial recognition**: Most important features are present, but some minor details or more secondary characteristics are missing or have being noticeable altered or newly added.

4 — **Strong recognition**: Recognizable, only some slight changes or addition in minor details have been done.

5 — **Perfect recognition**: Image is fully integrated with every minor detail conserved.

Aesthetics Score (0-5) — "Overall visual quality of the integration, if the integrated image has been synthetically inserted into the real life scenario."

0 — **Unusable**: The image has been copy and pasted directly onto a real life photo without any attention to perspective, illumination or basic coherence.

1 — **Very poor**: Despite some minor detail to give a more natural insertion, the image is still clearly inserted.

2 — **Poor**: Despite the details some key problems give away the synthetic insertion of the images.

3 — **Fair**: Insertion clear at first glance; acceptable composition; good enough to make doubt but has signs of synthetic insertion after a detailed observation.

4 — **Good**: Polished with only subtle imperfections, some minor illumination or perspective errors which make it difficult to discern if it was modified.

5 — **Excellent**: Impossible to discern if the image is original or was modified.

Alignment Score (0-5) — "How well adjusted is the information of a task prompt about the location of the integrated picture and what to extract."

0 — **Unusable**: Completely wrong location or completely wrong information about what to extract.

1 — **Very poor**: Difficult to understand or very ambiguous on what should be extracted.

2 — **Poor**: Somehow correct but confusing or ambiguous.

3 — **Fair**: Basic information without any class of details or additional information to deal with ambiguity.

4 — **Good**: Clear location and what to extract although some details are missing, leaving the possibility of some ambiguity.

5 — **Excellent**: Excellent information, clear and distinct leaving no room for ambiguity on what to extract.

TASK

Given the two images, one integrated into the other, and a task prompt with location information evaluate using the rubric; return the following JSON:

```
{
  "constancy_score": <integer 0-5>,
  "aesthetics_score": <integer 0-5>,
  "alignment_score": <integer 0-5>,
  "justification": 100-word explanation for each score
}
```

Figure 13. Prompt for scoring Synthetic WildSVG instances

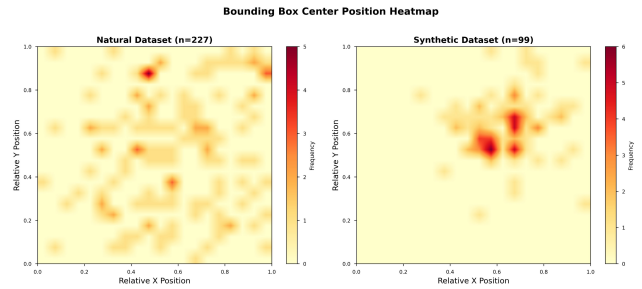


Figure 14. Bounding boxes position heatmap for WildSVG dataset test split

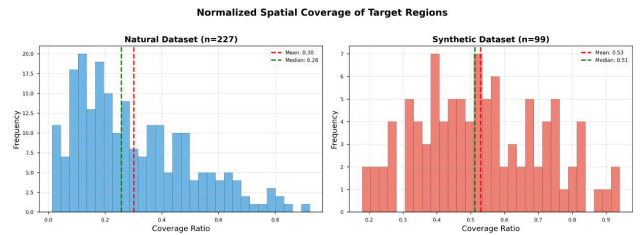


Figure 15. Distribution of bounding boxes coverage of the image for WildSVG dataset test split

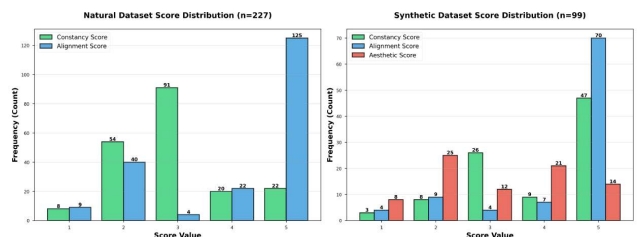


Figure 16. Score distribution for WildSVG dataset test split

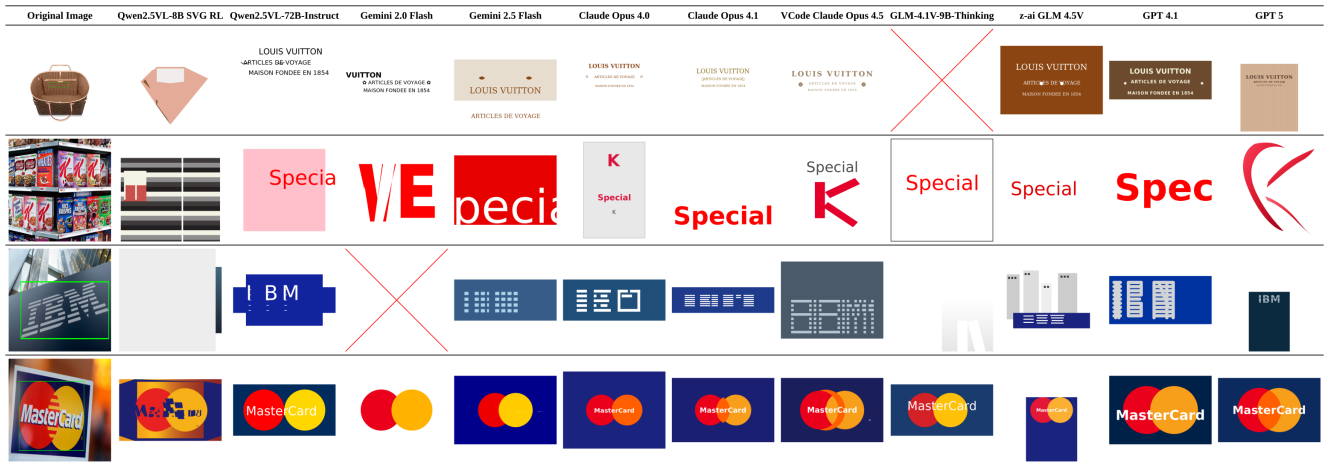


Figure 17. Comparison of VLMs for one-step SVG extraction natural dataset

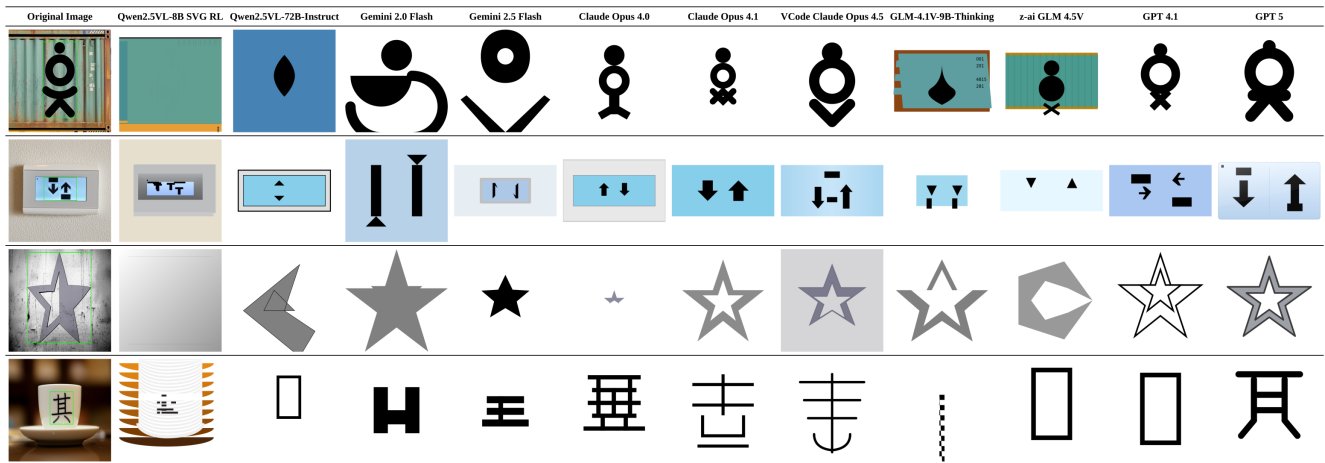


Figure 18. Comparison of VLMs for one-step SVG extraction synthetic dataset



Figure 19. Comparison of VLMs for two-step SVG extraction natural dataset



Figure 20. Examples of real-life images and associated SVG for natural WildSVG



Figure 21. Examples of real-life images and associated SVG for synthetic WildSVG